Study on Focusing Mechanism of Radial Polarization with Immersion Objective

2008 Jpn. J. Appl. Phys. 47 5806

(http://iopscience.iop.org/1347-4065/47/7S1/5806)

Japanese Journal of Applied Physics
Vol. 47, No. 7, 2008, pp. 5806–5808

Study on Focusing Mechanism of Radial Polarization with Immersion Objective

Tzu-Hsiang LAN* and Chung-Hao TIEN[1]

Department of Photonics and Institute of Electro-Optical Engineering, National Chiao Tung University, Hsinchu 300-10, Taiwan
[1]*Department of Photonics and Display Institute, National Chiao Tung University, Hsinchu 300-10, Taiwan*

(Received December 1, 2007; accepted March 3, 2008; published online July 18, 2008)

In this study, we employ vectorial diffraction to examine the focusing mechanism of radially polarized beams using an immersion objective with linear and circular polarized illuminations. Radial polarization features a sharp focus in a high-numerical-aperture (NA) system. The longitudinal component governing spot formation depends on the bending of the polarization vector rather than the immersion circumstance. As the marginal angle of the objective exceeds 64.16 and 71.81°, the depolarization effect of the radially polarized beam enables a smaller spot than the linear and circular polarizations, respectively. [DOI: 10.1143/JJAP.47.5806]

KEYWORDS: radial polarization, immersion objective, marginal angle, refraction index, high numerical aperture, optical data storage system

1. Introduction

It is well known that the focus spot in optical data storage (ODS) systems is determined by the scalar diffraction $\sim k\lambda/\mathrm{NA}$, where λ is the free space wavelength and NA is the numerical aperture of the objective lens. The factor k is of the order unity and depends on apodization. In order to produce the smallest possible spot, it is desirable to pursue shorter wavelengths and higher NAs. However, the characteristics of vectorial behavior would be more apparent in a high-NA system and lead to an unsymmetrical focus (called elongation effect) under linear polarized illumination.[1)]

Recently, a doughnut-shaped optical field obtained via radial polarization (RP) attracted much attention owing to the preservation of the symmetric property of the focused spot. Such a unique feature makes it possible to apply RP in high resolution systems.[2–5)] Several methods have been proposed to generate such as axially symmetric polarized beam. Generally, the formation can be classified into two types. One directly generates the beam from the laser cavity,[6)] the other approach involves indirect generation outside the laser cavity using the interference of two orthogonal Hermite–Gaussian modes.[7,8)]

On the other hand, immersion technologies such as solid-immersion lens (SIL) yielding an effective NA ($\mathrm{NA_{EFF}}$) above 1.0 also provide a route for radially polarized beams.[9,10)] In a SIL system the longitudinal component of focused radially polarized beams dominates the lateral size of the focus spot and propagates through the interface around 5–6 wavelengths.[11–13)] In addition, the optical aberration caused by the air spacing can be alleviated owing to the characteristics of cylindrical symmetry.

On the basis of the above mentioned features, we neglected the spherical aberration caused by air spacing and selected water as the immersion medium. The focus spot was observed in the immersion medium, and the comparisons of the focus spot with other homogeneous polarization modes were also carried out.

2. Simulation

An ideal aplanatic system with a focusing power $\lambda/\mathrm{NA_{EFF}}$ is discussed, where $\mathrm{NA_{EFF}} = n \times \mathrm{NA_{AIR}}$ (n: refractive index of the focusing medium. $\mathrm{NA_{AIR}}$: focused light in a dry lens which entirely depends on its angle of marginal ray). Figure 1 schematically shows the states of polarization on the pupil: (a) linear, (b) circular, and (c) radial polarizations, respectively. Ei and Eo represent the electric field before and after passing through the objective. The electric component at focus can be decomposed into two orthogonal components: transversal ($I_{\mathrm{trans}} = I_X + I_Y$) and longitudinal ($I_{\mathrm{long}} = I_Z$) components. Figure 2 shows the intensity and phase distribution at focus for RP with $\mathrm{NA_{EFF}} = 1.33$ ($n = 1.33$ with $\mathrm{NA_{AIR}} = 1$), where I_X, I_Y, and I_Z denote the decomposed intensity distribution, and P_X, P_Y, and P_Z represent the corresponding phase plots for E_X, E_Y, and E_Z.

The phases P_X and P_Y reveal the acquired curvature of the beam, as well as the π-phase difference between the two halves of E_X and E_Y. Whereas E_X and E_Y take the square operation, the two fold symmetry of I_X and I_Y result from the phase singularity along the y- and x-axes. The shape of the intensity distribution depends on individual phase distributions.

Unlike the elongation effect from linear polarization (LP), the phase pattern P_Z of the longitudinal component of RP has concentric circles with a converging wavefront. The appreciable longitudinal component would result in a focus spot with cylindrical symmetry. Likewise, the longitudinal component of circular polarization (CP) shows a central hole in the intensity distribution caused by a continuous variation from 0 to 2π around the vortex. This donut-shaped intensity of longitudinal component ensures that the shape of the focus spot is also cylindrical with a slight spread.

3. Discussion

3.1 Decomposition of focus spot

In order to further investigate the focusing mechanism of RP associated with the immersion objective, an aplanatic focusing model was introduced, as shown in Fig. 1. We define a ratio of the longitudinal to transversal component as follows:

$$\text{L–T ratio} \equiv \frac{\text{Peak intensity of } \textit{longitudinal} \text{ component}}{\text{Peak intensity of } \textit{transversal} \text{ component}}.$$

Figure 3 shows the different L–T ratios of focused RP in water: (a) L–T ratio = 0.81, (b) L–T ratio = 1.38, and (c) L–T ratio = 2.94. The black solid, black dashed, and

*E-mail address: allenblue.eo94g@nctu.edu.tw

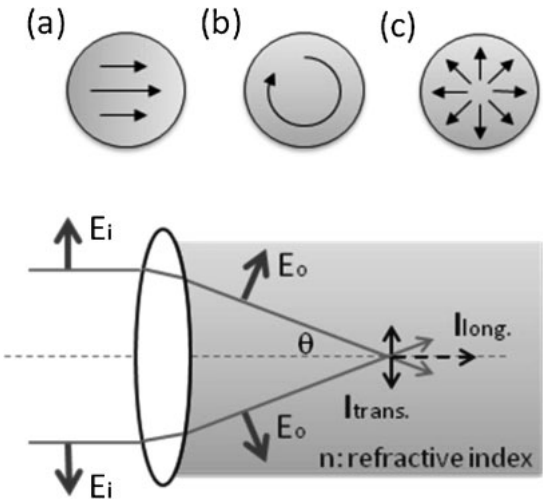

Fig. 1. Schematic diagram of aplanatic focusing model and different illumination beams: (a) linear, (b) circular, and (c) radial polarizations, where Ei and Eo represent electric field of radial polarization, and I_{long} and I_{trans} represent the decomposed intensity distribution.

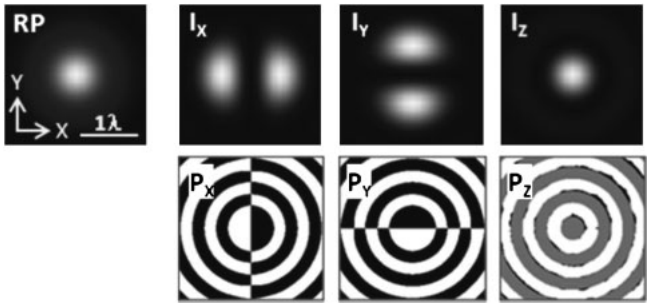

Fig. 2. Intensity and phase distribution of field distribution in focus with $NA_{AIR} = 1.0$ for RP. I_X, I_Y, and I_Z denote the decomposed intensity distribution and P_X, P_Y, and P_Z represent individual phase distributions.

gray dashed lines represent the intensity curve of total, longitudinal, and transversal components, respectively. As the L–T ratio increases, the shape of the focus spot changed from a donut-shaped spot to a circular spot. The flat-topped shape shown in Fig. 3(b) with a L–T ratio = 1.38 is at the transition midway between above two cases. Once the L–T ratio becomes larger than the critical value, the dip in field intensity disappears; therefore, the beam shape is centralized by the considerable longitudinal component.

It must be mentioned that a high L–T ratio ensures that RP produces a smaller focus spot. The marginal angle determines the projection power of the transversal component onto the longitudinal component. That is, for RP, the shape of the focus spot entirely depends on the bending of the polarization vector, and the refractive index merely functions as a proportional scale factor.

Figure 4 shows two L–T ratio curves for focusing RP with $n = 1.0$ (dashed line) and $n = 1.33$ (solid line). The subfigures of focus spot correspond to specific L–T ratios. Drawing a line parallel to the x-axis at L–T ratio = 1.38 separates those subfigures into two parts: donut-shaped and circular focus spots. Two lines exhibit a common L–T ratio 5.16 at $NA_{EFF} = 1.0$ and 1.33 for different immersion media. The maximum solid angle of a single objective is 2π, which limits the strength of the longitudinal component

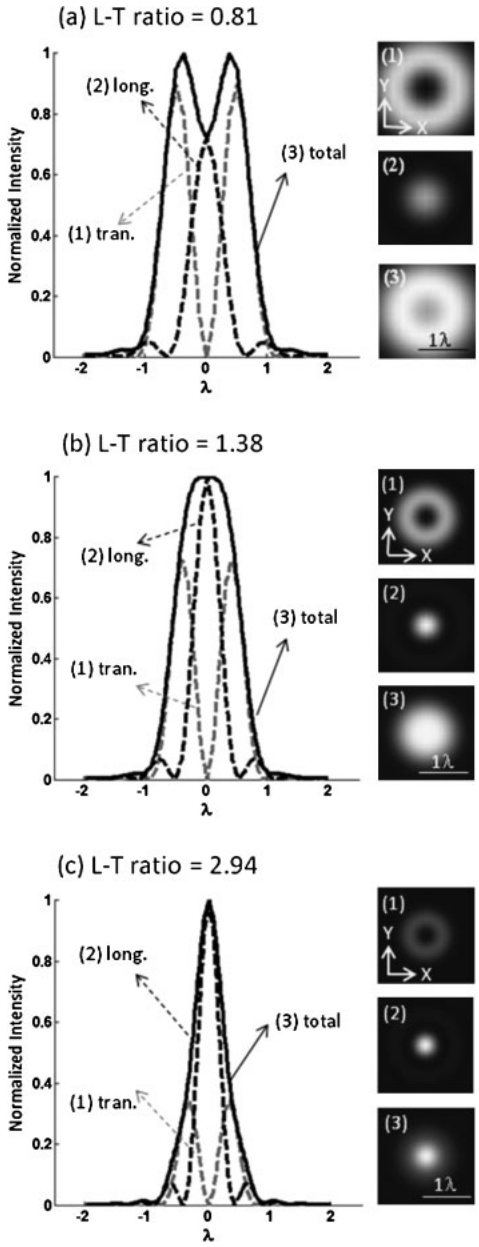

Fig. 3. Different L–T ratios with calculated cross section and two-dimensional field distribution in focus for RP beam focused by water immersion objective: (a) L–T ratio = 0.81, (b) L–T ratio = 1.38, and (c) L–T ratio = 2.94.

projected from the transversal component. In addition, as the NA_{EFF} of the solid line is divided by the refractive index 1.33, the new line is identical to those reported in the literature.[9)]

3.2 *Comparison of full width at half maximum*

Owing to the high L–T ratio, the shape of total field distribution at a high NA will mainly be governed by the longitudinal component. With reference to Fig. 5, we discuss the full width at half maximum (FWHM) of the focusing spot in various states of polarization and immersion media. Since the refractive index of the immersion medium only provides a proportional down-scale factor, here we only address the case in air for simplicity.

Recall the L–T ratio = 1.38 shown in Fig. 3(b), whereas $NA_{EFF} > 0.73$, the longitudinal to transverse component of

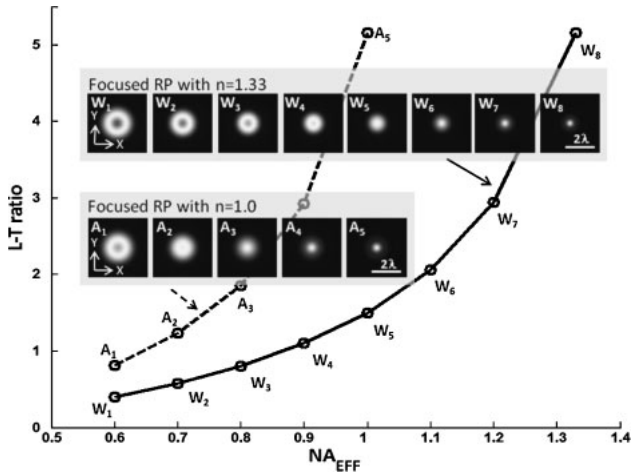

Fig. 4. L–T ratio of RP in focus vs NA_{EFF} focused with dry lens and water immersion objective.

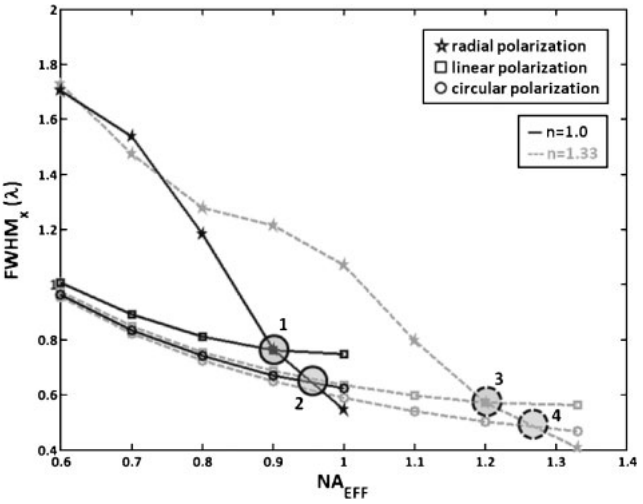

Fig. 5. Comparison of $FWHM_x$ (measured along x-axis) vs NA_{EFF} for different illumination beams. The black and gray lines represent the focused light in air ($n = 1.0$) and water ($n = 1.33$), respectively. The lines with symbols represent different beams (□: linear polarization, ○: circular polarization, ★: radial polarization).

the optical field has a critical ratio at which the optical field is transformed from a donut-shaped to a flat-topped shape. After that, the depolarization effect starts to govern the formation of the focused spot. As NA_{EFF} increases, the FWHM of RP exhibits a faster reduction and comparable to LP and CP at NA_{EFF} higher than 0.9 and 0.95, respectively. It was noted that superior radial illumination only exists in a high marginal ray. Compared with LP and CP, the smaller spot obtained by RP was under the conditions of marginal angle $> 64.16^\circ$ (mark 1) and marginal angle $> 71.81^\circ$ (mark 2), respectively. Likewise, in the case of using water similar results (mark 3 and mark 4) were obtained considering the effect of refractive index.

Another issue that must be addressed is that for LP, a discrepancy in FWHM exists under different immersion media. The faster spot size reduction in water is due to refractive index acting as a buffer to retard a considerable elongation effect caused by the longitudinal component as $NA_{EFF} > 0.6$. CP provides a good focus shape with no elongated aberration in a wide marginal angle from 0 to 71.8°. Although focused RP can generate the smallest focus spot, the required maximum marginal angle should be larger than 71.8°; also the design and cost of this type of lens are complex and expensive. Therefore, these features restrict the applicability of RP.

4. Conclusions

In this paper, we examined the focusing mechanism of radially polarized beam associated with the immersion technology and compared the focus spot between linear and circular illuminations. According to our numerical analyses, the refractive index of the immersion medium only provides a proportional scale factor and does not involve enlarge event of the longitudinal component of RP. The degree of marginal angle is the key issue for RP to form a small focus spot. As the marginal angle of the objective exceeds 64.16 and 71.81°, the high L–T ratio of the RP enables the formation of a smaller spot than LP and CP, respectively. In an optical focusing system, CP is widely adopted, but RP provides a niche market in some applications.

Acknowledgement

This work was supported by the National Science Council, Republic of China under Contract No. NSC96-2752-E009-009-PAE.

1) M. Mansuripur: J. Opt. Soc. Am. A **6** (1989) 786.
2) S. Quabis, R. Dorn, M. Eberler, O. Glöckl, and G. Leuchs: Opt. Commun. **179** (2000) 1.
3) R. Dorn, S. Quabis, and G. Leuchs: Phys. Rev. Lett. **91** (2003) 233901.
4) W. C. Kim, N. C. Park, Y. J. Yoon, H. Choi, and Y. P. Park: Opt. Rev. **14** (2007) 236.
5) T. H. Lan and C. H. Tien: Jpn. J. Appl. Phys. **42** (2007) 3758.
6) Y. Kozawa and S. Sato: Opt. Lett. **30** (2005) 3036.
7) B. Jia, X. Gan, and M. Gu: Opt. Express **13** (2005) 6821.
8) S. C. Tidwell, D. H. Ford, and W. D. Kimura: Appl. Opt. **29** (1990) 2234.
9) K. S. Youngworth and T. G. Brown: Opt. Express **7** (2000) 77.
10) C. J. R. Sheppard and A. Choudhury: Appl. Opt. **43** (2004) 4322.
11) P. Török, P. Varga, and G. R. Booker: J. Opt. Soc. Am. A **12** (1995) 2136.
12) D. P. Biss and T. G. Brown: Opt. Express **9** (2001) 490.
13) L. E. Helseth: Opt. Commun. **191** (2001) 161.